Depositional Environment and Lithofacies Variability of the Austin Chalk: Identification of a Prolific New South Texas Horizontal Play Based on Analyses of Drill Cuttings

By

Alec Veasey

Department of Geosciences, UTD – Fall 2022

Supervisors: Dr. Robert J. Stern

Mr. Lowell Waite

Abstract

The Late Cretaceous was a unique time in Earth's history. Poorly circulated oceans, ocean anoxic events, and large nutrient influxes brought on by increased volcanism led to widespread deposition and burial of organic-rich mudrocks that have sourced some of the largest oil and gas fields in the world. Recently the Austin Chalk has emerged as a prolific horizontal play in South Texas. The Austin Chalk is part of the Gulfian Series deposited during the Coniacian- Early Campanian interval. The purpose of this research involves the utilization of Loucks's (2020) analysis of Austin Chalk cores spanning the underlying Stuart City reef trend and applying his facies scheme to drill cuttings obtained from two producing wells in south Texas. The region of study occurs down-dip of the Stuart City margin, in a region characterized by a Late Cretaceous submarine plateau, between the Rio Grande Embayment and the Maverick Basin. The goal of the study is to document the best zones of production within the Austin Chalk and demonstrate how application of readily available tools within academia can help industry. Age interpretation based on nannofossil biostratigraphy of a well in the study area documents that the best target zone resides within the lowermost portion of the chalk in an interval coinciding with the Late Coniacian Carbon Isotope Excursion Event (LCIE) within the lower portion of the global OAE3 event. XRD and XRF analysis of drill cuttings were applied to better understand the mineralogical differences and define geochemical signatures of the different lithofacies assigned by Loucks. Elemental proxies were used to account for anoxia and

productivity present in the cuttings. XRF analysis of cuttings from a lateral well in the study area was employed to help locate faults that are rarely encountered in core, due to their tendency to occur at a high angle of dip. The lateral targeting of these faults within zones of the Austin Chalk that reside within the LCIE would likely be economically beneficial.

Table of Contents

Introduction……. 4

Depositional Environment…… 4-6

Lithofacies of the Austin Chalk …….. 6-7

Study Area & Biostratigraphy…… 7-8

Methods……. 8-9

Drill Cuttings/XRD Analysis (State Mary 4H) ……. 9-10

XRF Analysis (State Mary 102H)……. 10-11

Conclusions…….. 11-12

References……. 12-13

Figures……. 14-20

Introduction

Approximately 50% of the largest oil fields exploited today were sourced during the Late Cretaceous Zuni Megacycle (Klemme and Ulmishek, 1990). The Austin Chalk was deposited during the 2nd order Zuni 3 sea-level cycle. The Austin Chalk is part of the Gulfian Series of the Upper Cretaceous, a deep-water carbonate that was deposited throughout the northern Gulf of Mexico Basin during the Conacian – Early Campanian interval on a drowned Late Cretaceous paleo shelf. The Austin Chalk is a prominent petroleum reservoir, widely considered to be a fracture play for the oil and gas industry and has recently emerged as a prolific horizontal play in south Texas. For this study, drill cuttings from two producing wells in Webb County, Texas, were provided by a local Dallas oil company. One well was drilled vertically through the Austin Chalk before landing in the Eagle Ford, while a second well was drilled laterally through the lower portion of the Austin Chalk. An overall visual description of the drill cuttings is provided along with X-Ray Diffraction (XRD) mineralogical, and X-Ray Fluorescence (XRF) chemical analyses. The purpose of this research was to better understand lithofacies variation and depositional environment of the Austin Chalk in Webb County, Texas, in order to identify the best zones of production. XRD and XRF analysis of the cuttings was used to better understand the mineralogical differences between facies and for fault identification. This study demonstrates how academia and industry can come together to make new discoveries, with scientific instruments commonly available at universities.

Regional Depositional Setting of the Austin Chalk

The Cretaceous was a unique time in Earth's history that lasted 69 million years, from 145 to 66 Ma, and marks the closing chapter of the Mesozoic Era. The Cretaceous in North America is known for the opening of the Western Interior Seaway (WIS), where a shallow sea drowned the central portion of the continent. Significant seafloor spreading occurred during the Cretaceous from 120 to 80 Ma, believed to be the consequence of increased magmatic activity and generation of a "superplume" that was located in the modern-day Pacific Ocean (Larson, 1991). The opening of the WIS is believed to be controlled by a combination of subsidence and eustatic sea-level rise due to the displacement of water by young oceanic lithosphere generated at the spreading ridges. The driving force for the subsidence throughout the middle of North America remains speculative. Some researchers have suggested the slab pull force of the subducting Farallon plate from the southwestern margin of North America created the subsidence needed to force drowning of the western interior of North America (Liu, 2015), leading to the large-scale deposition of Late Cretaceous deep-water carbonates.

Cretaceous oceans did not resemble oceans of the modern world (Hay, 2008). Cretaceous oceans were poorly oxygenated and more stagnant, leading to widespread occurrence of anoxic bottom waters and the formation of large scale Oceanic Anoxic Events (OAEs). There are three documented OAEs for the Cretaceous. The youngest of these, OAE 3, took place during the Conacian-Santonian interval during deposition of the Austin Chalk. OAEs

are thought to be one of the main contributing factors for the deposition and preservation of large amounts of organic matter in the world's oceans. An increase in ratios of carbon 13 to carbon 12 is noted during the Late Coniacian. This event was named the Late Coniacian Carbon Isotope Excursion Event (LCIE) (Lowrey et al., 2017).

Continental arc magmatism was prevalent along the western margin of North America during the Late Cretaceous. The origin of numerous ash beds within the upper Austin Chalk has been a topic of debate among geoscientists. The presence of nearby submarine volcanoes was once believed to be the source of the bentonite beds in the Austin Chalk. A detailed study conducted on bentonite beds of the Austin Chalk in Dallas County, however, revealed a more distant source, most likely originating from continental arc magmatism of the western margin of the United States (Collins, 1979). The presence of volcanic quartz in the chalk further supports the hypothesis of distant arc volcanism, due to the fact that volcanic features in South Texas are silica-poor. A recent study found that an increase in volcanism during the Late Cretaceous led to a large global flux of nutrients derived from windblown volcanic ash (Lee et al., 2018). This increase in nutrients from Cretaceous ash enhanced biological productivity and increased burial rates, resulting in vast amounts organic carbon preservation during the deposition of the Late Cretaceous Gulfian Series.

Lithofacies of the Austin Chalk

Loucks et al. (2020) analyzed Austin Chalk cores spanning the trend of the underlying Lower Cretaceous Stuart City reef, from South Texas to Louisiana. His analysis of multiple cores

showed five common lithofacies (Fig.1), with vertical variations in lithofacies from less than a foot to meters in scale (Loucks et al. 2020). These lithofacies reflect the oxygen content of the WIS during deposition, documenting a transition from oxic to more dysoxic Cretaceous bottom waters. The lithofacies in the Austin Chalk range from a marly chalk to chalky marl. Lithofacies one through four show indicators of increasing anoxic conditions at time of deposition, with lithofacies one being the most oxic. Decreasing bioturbation with increasing laminations and pyrite content is characteristic of facies three and four. The average Total Organic Carbon (TOC) of the cores increases with increasing anoxic markers. Lithofacies five represents debrites derived from gravity flows and is only found in updip areas of the chalk. Average mineralogy of the cores varies based on location and depth along the Stuart City Reef trend. A goal of the current study was to use Loucks's facies definitions derived from core analysis and apply his scheme to drill cuttings in the absence of cores.

Study Area & Biostratigraphy

Drill cuttings were obtained from two producing wells in Webb County, Texas. Both wells were drilled downdip of the underlying Stuart City reef margin, in a locally deeper-water region or submarine plateau known as the Rio Grande Submarine Plateau, located between the Stuart City reef and the Sligo reef trends (Hancock, 2019; Fig.2C). These two wells were drilled in a deeper sub basin than any of Loucks et al. (2020) cores spanning the Stuart City reef trend. The Austin Chalk in Webb County currently reside in the dry gas thermal window (Zumberge et al., 2016).

Biostratigraphic data was available for a nearby well in Webb County (Fig.3). An age interpretation was made based on the occurrence of calcareous nannofossils. Analysis of the data defines the stratigraphic position of OAE 3 and the LCIE in the well; it also shows the presence of a significant unconformity defining a major a sequence boundary at the Santonian-Campanian stage boundary, where Late Santonian deposits are missing (Fig. 3). This sequence boundary is seen as a dramatic spike on the gamma ray log. Lithostratigraphic correlation of the biostratigraphic zones to the two study wells shows that the LCIE falls within the lower portion of the Austin Chalk. This lower portion of the chalk is commonly referred to as Zone D (Ewing, 2013). Zone D represents the most organic-rich portion of the Austin Chalk with an abundance of lithofacies four. This represents the main target zone of the horizontal study well.

Methods

An initial visual description of well cuttings from the vertical was conducted first. The Austin Chalk interval samples were cleaned and submerged in water for better viewing under low magnification using a binocular microscope. The samples were placed in trays and aligned based on the measured drilling depth in feet (Fig 4). After the initial description, the cuttings from the vertical well were further analyzed utilizing the UTD Geoscience Department's Thermo Scientific ARL Equinox 100 X-Ray Diffractometer (XRD) instrument. Before running the samples through the XRD, they had to be pulverized and sieved utilizing a U.S.A Standard Testing No. 80, 180 micrometer opening sieve. After running the cuttings through the XRD machine, match

software was utilized to find best fit of match (FOM). Well cutting samples from the horizontal well were prepared in a different manner for XRF analysis. In this case the drill cuttings were ground with a mortar and pestle and compressed into flat cylindrical disks, to acquire more accurate elemental data utilizing the department's handheld Thermo Scientific Niton XL3 Analyzer XRF device (Fig 5). Great care was taken to minimize contamination of the samples during both XRD and XRF analysis. The data on the wells was collected and analyzed through the use of simple cross-plots and diagrams.

Drill Cuttings/XRD Analysis of the Vertical Well Samples

Descriptions of drill cuttings from the vertical well were plotted next to the existing mudlog (provided by the operator) for a more accurate placement of the visual descriptions (Fig 6). Zonation of the Austin Chalk (shown in green) is based on Ewing's work in 2013, utilizing the gamma ray curve for correlation. Abundant free calcite was seen in the top of the Austin Chalk at 11,650'MD, interpreted as derived from abundant calcite sealed fractures. The free calcite disappeared in the cuttings at 11,775'MD, coinciding with a significant increase in clay content and representing the Kickoff Point (KOP) for the horizontal portion of the well. The most organic-rich sample was seen at 11,900'MD. The cuttings show a general increase in both organic richness and pyrite content with depth. Pyrite framboids replace the calcareous tests of some fossils in some samples. The top of the Cenomanian – Turonian Eagle Ford Formation occurs at a measured depth of 12,150', denoted by a strong increase in both organic richness and free pyrite. The horizontal target zone for horizontal well is shown in bright red on Figure 6.

A summary of XRD analysis of cuttings from the vertical well is displayed in Fig 7. Calcite is shown with a blue line, quartz is shown with a yellow line, beryllium fluoride is shown with a white line, and unidentified peaks are shown with a pink line. The unidentified peaks are likely due to the XRDs inability to properly identify clay minerals. The beryllium fluoride is interpreted to be cristobalite, a high temperature polymorph of quartz. The XRD software likely assigned beryllium fluoride instead of quartz due to similarities in their structure. The presence of cristobalite implies a volcanic origin for the quartz. An area with a drop in calcite and an increase in quartz and clay minerals was also noted. These changes occur in the clay-rich interval with abundant quartz at the KOP on the mud log at 11,775'MD (Fig 8). This depth corresponds exactly to the Campanian-Santonian unconformity . The steep drop in quartz could be due to the decrease in volcanism, or may have a biogenic origin, as it correlates to the upper boundary of OAE 3 (Fig 8).

The XRD data was correlated to the mudlog for the vertical well for a better understanding of mineralogical changes with depth (Fig 9). Since bioturbation and laminations are not normally observed in drill cuttings, assignment of Loucks (2020) lithofacies were made on the basis of geochemical markers. It was found that the XRD was not sufficiently accurate in defining elemental changes, due to the inability of the instrument to detect clays. The XRD's reliability on match software databases is another challenge. It was therefore determined that the elemental analysis of the drill cuttings for the horizontal well required XRF analysis.

XRF Analysis of the Horizontal Well

Drill cuttings from the horizontal well were analyzed with an XRF multiple times to get a better understanding of the data and to check for both instrument and human errors The data was compiled in the form of graphs including the well trajectory from the geosteering report provided by the operator (Fig 10). The target zone (Zone D) is shown in green, with total gas for the well shown at the top of the diagram in red. Calcium (blue line), silica (yellow line), and aluminum (Green Line) are shown in weight percent. The presence of a fault, interpreted from seismic data (not shown) is marked by a rapid increase in both aluminum and silica.

Silica and aluminum peaks together may indicate an increase in organic-rich material, indicating that the fault displaced the formation, putting the lateral wellbore in a more organic-rich portion of the chalk. This interpretation is confirmed in the horizontal well cuttings which show a distinct change to a darker gray color at the interpreted fault. Vanadium (purple line), copper (orange line), and nickel (brown line) contents are shown in parts per million (ppm) and were used as elemental proxies for productivity and anoxia (Fig 11). An estimate of productivity is displayed under total gas to show zones where geochemical productivity markers are highest. Two addition faults were interpreted on the seismic data towards the toe of the lateral well and correspond directly with a sudden change in amount of these elements, in addition with the spikes in total gas. Molybdenum (teal line) and thorium (black line) amounts are shown in ppm (Fig 12). Molybdenum is another reliable proxy for anoxia. Loucks et al. (2020) found that thorium was found in abundance in the clay-rich layers of the Austin Chalk. The sudden changes of peaks in these elemental proxies line up with large peaks in gas, providing further evidence for the presence of a graben-like fault structure in this portion of the lateral well.

Loucks et al. (2020) showed that pyrite content increases from lithofacies one through four. Pyrite is an iron sulfide (FeS_2) and utilizing XRF data, both iron (red line) and sulfur (yellow line) were plotted against the trajectory of the horizontal wellbore (Fig 13). The XRF data shows an increase of both

elements within areas of high productivity. Pyrite content in the different lithofacies remains fairly constant along cores spanning the Stuart City reef trend (Loucks, 2020). Increased amounts of iron and sulfide in downdip regions of the Austin Chalk using XRF analysis may provide a relatively quick and inexpensive method of identifying potential productive lithofacies when working with drill cuttings.

Conclusions

Loucks (2020) research showed that mineralogy of the different Austin Chalk lithofacies was variable along the underlying Stuart City reef trend. The two producing wells of the present study were deposited in a deeper sub-basin compared to the cores studied by Loucks (2020) and could account for observed mineralogical differences . Bioturbation and laminations are not observable in drill cuttings, and therefore, lithofacies characterization of cutting must be based on geochemical analysis. Biostratigraphy of a nearby well in the study area shows that the main horizontal target zone for the Austin Chalk (zone D) is time equivalent to the LCIE, which contains the most organic-rich portion of the Austin chalk with an abundance of lithofacies three and four. The Austin Chalk is a fracture play, with interpreted faults aligning with large peaks in total formation gas. Future wells in the area targeting these faults would be economically beneficial in the production of gas. Pyrite content and elemental proxies for productivity and anoxia based on XRF analysis of drill cuttings provides a relatively rapid, inexpensive way to assign lithofacies and identify possible highly productive zones within the Austin Chalk. Vital economic information from drill cuttings can therefore be obtained utilizing scientific instruments available at universities, highlighting the benefits of academic – industry collaboration.

Acknowledgements

We wish to thank an oil company who wishes to remain anonymous for access to well samples and other geologic information which made this study possible.

References

Blakey, R. C, 2014, Paleogeography and Plate tectonics of the Western Interior Seaway, Jurassic-Cretaceous of North America: Search and Discovery Article #30392, posted December 29, 2014.

Collins, J. R, 1979, Characteristics and Origin of the Cedar hill bentonite bed, lower Austin Chalk, Dallas County vicinity, ISBN-13: OCLC:37747016.

Durham, C. O, Hall, S. H, 1991, The Austin Chalk; Bed by bed through central Texas, Geology, geophysics, and formation evaluation. South Texas Geological Society.

Ewing, T. E., 2013, Stratigraphy of the Austin, Eagle Ford, and Anacacho formations and its influence on hydrocarbon resources, Pearsall Field area, South Texas: Gulf Coast Association of Geological Societies Transactions, v. 63, p. 213– 225.

Hancock, A.M., 2019, Evaluation of subsurface porosity in the Austin Chalk Group, south Texas; unpublished M.S. Thesis, University of Texas at San Antonio, 84 p.

Hay, W. W., 2008, Evolving ideas about Cretaceous climate and ocean circulation: Cretaceous Research, v. 29, p. 725-753.

Klemme, H.D., and Ulmishek, G.F., 1990, Effective petroleum source rocks of the world: Stratigraphic distribution and controlling depositional factors: AAPG Bulletin, v.75, p. 1809-1851.

Larson, R. L., 1991, Latest pulse of earth: Evidence for a mid-Cretaceous superplume: Geology, v. 19, no. 6, p. 547, doi:10.1130/0091-7613(1991)019<0547:lpoeef>2.3.co;2.

Lee, C.-T. A., H. Jiang, E. Ronay, D. Minisini, J. Stiles, and M. Neal, 2018, Volcanic ash as a driver of enhanced organic carbon burial in the cretaceous: Scientific Reports, v. 8, no. 1, doi:10.1038/s41598-018-22576-3.

Liu, L., The ups and downs of North America: Evaluating the role of mantle dynamic topography since the Mesozoic, Rev. Geophys., 53, p. 1022–1049, doi:10.1002/2015RG000489.

Loucks, R. G., Lambert, J. R., Patty, K., Larson, T. E., Reed, R. E., Zahm, C. K., 2020, Regional Overview and Significance of The Mineralogy of the Upper Cretaceous Austin Chalk Group, Onshore Gulf of Mexico, Gulf Coast Association of Geological Societies, GCAGS Journal, V.9 (2020), p 1-16

Loucks, R. G., R. M. Reed, L. T. Ko, C. K. Zahm, and T. E. Larson, 2021, Micropetrographic characterization of a siliciclastic-rich chalk; Upper Cretaceous Austin Chalk Group along the onshore northern Gulf of Mexico, USA: Sedimentary Geology, v. 412, p. 105821, doi:10.1016/j.sedgeo.2020.105821.

Loucks, R. G., T. E. Larson, C. Y. C. Zheng, C. K. Zahm, L. T. Ko, J. E. Sivil, P. Sheng, S. C. Ruppel, and W. A. Ambrose, 2020, Geologic characterization of the type cored section for the upper cretaceous Austin Chalk Group in southern Texas: A combination fractured and unconventional reservoir: AAPG Bulletin, v. 104, no. 10, p. 2209–2245, doi:10.1306/04222019197.

Loucks, R. G., and R. M. Reed, 2022, Implications for carbonate mass-wasting complexes induced by volcanism from Upper Cretaceous austin chalk strata in the Maverick Basin and San Marcos Arch areas of south-Central Texas, USA: Sedimentary Geology, v. 432, p. 106120, doi:10.1016/j.sedgeo.2022.106120.

Lowery, C. M., R. M. Leckie, and B. B. Sageman, 2017, Micropaleontological evidence for redox changes in the OAE3 interval of the US western interior: Global vs. local processes: Cretaceous Research, v. 69, p. 34–48, doi:10.1016/j.cretres.2016.08.011.

Zumberg, J. Illich, H., and Waite, L. 2016, Petroleum geochemistry of the Cenomanian – Turonian Eagle Ford oils of south Texas, *in* Breyer, J.A., The Eagle Ford Shale: A renaissance in U.S. oil production: AAPG Memoir 110, p. 135-165.

Figures

Figure 1. The Austin Chalk lithofacies described by Loucks. These lithofacies were based on cores samples of the Austin Chalk spanning the Stuart City reef trend. Figure modified from (Loucks et al. 2021).

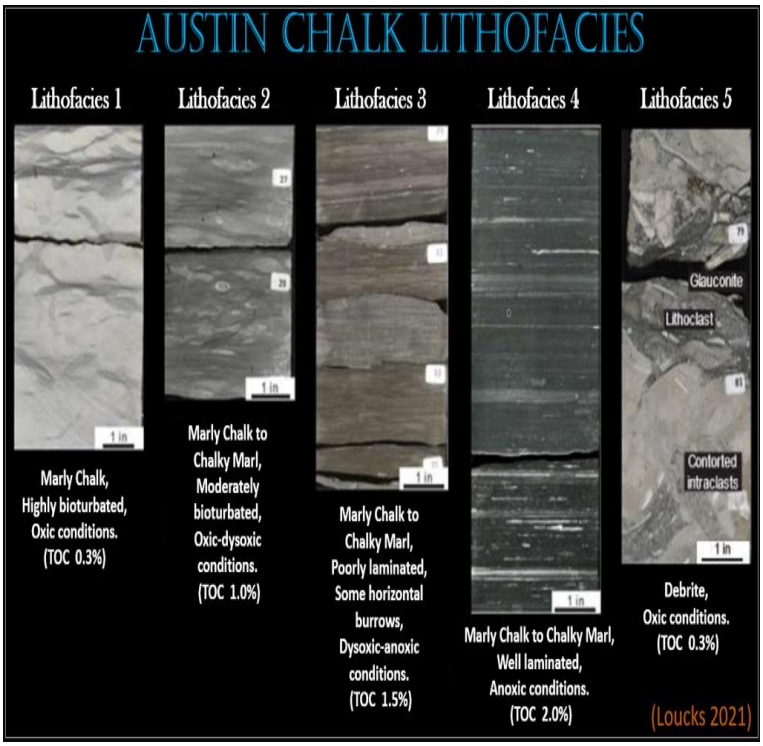

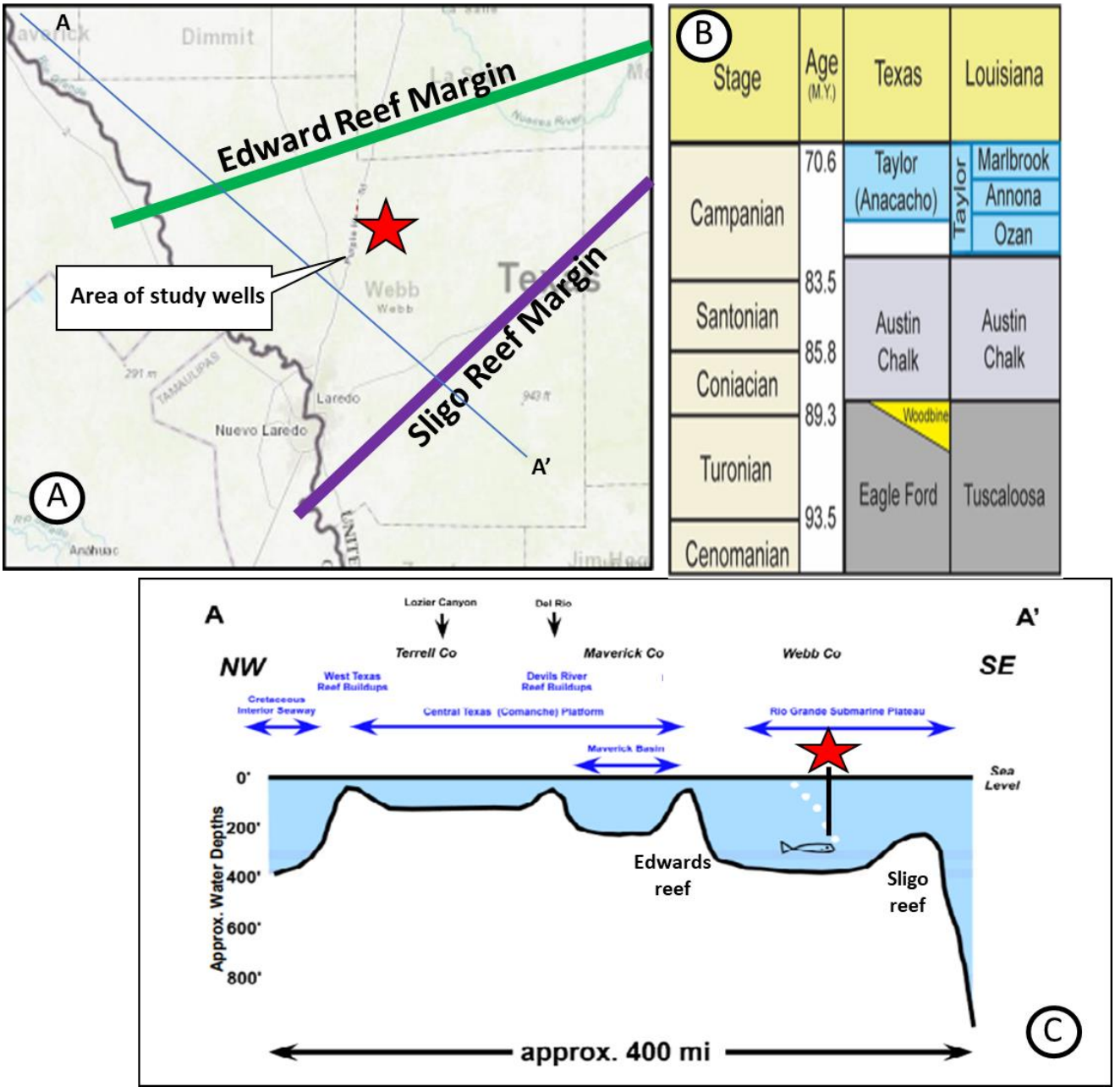

Figure 2. Overview of the study area in Webb County. A) General location of vertical and horizontal study wells in Webb Co., Texas (shown by red star); cross-section A-A' shown in panel 2C. B) Late/Upper Cretaceous chrono- and lithostratigraphic units of the northern Gulf Coast Basin showing stratigraphic position of the Austin Chalk (from Loucks, 2020 and other sources). C) General NW-SE cross section

across region showing the study area (red star) resides in the deep-water Rio Grande submarine plateau, between the buried Stuart City/Edwards and Sligo reef trends; location of cross-section shown in panel 2A (modified from Hancock, 2019).

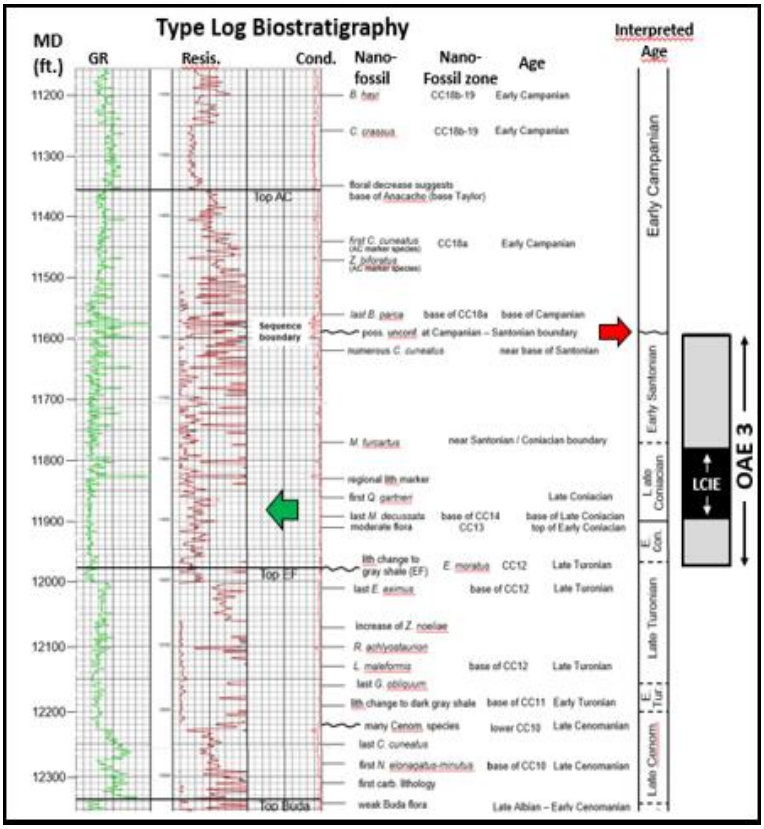

Figure 3. Biostratigraphy of the nearby well, from a report provided by the operator. Age interpretation is based on the presence of calcareous nannofossils. An unconformity was found at an interpreted sequence boundary, shown with a red arrow. At this boundary, sediments of Late Santonian age are missing. The LCIE within the greater OAE 3 are also shown. The green arrow depicts the approximate landing zone (zone D) of horizontal well, which resides entirely within the LCIE, the most organic-rich portion of the Austin Chalk.

Figure 4. Drill cuttings from the vertical well, washed and prepared in trays with interval and scale labeled. The Austin Chalk (top left) begins a depth of 11,650’ MD(measured depth) and ends at the top of the Eagle Ford at 12,150’MD (bottom right).

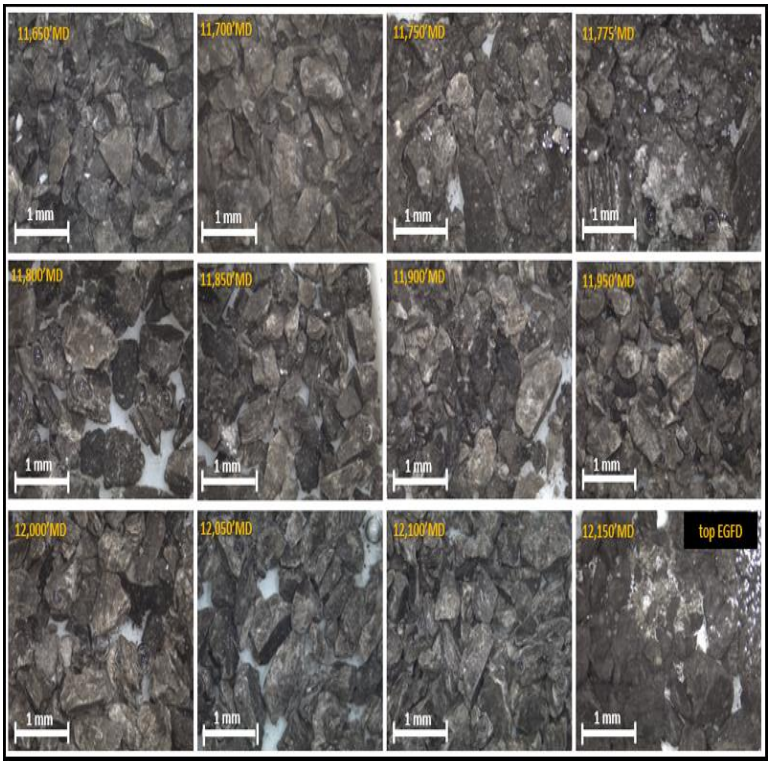

Figure 5. Drill cuttings from the horizontal well, ground and pressed in cylindrical disks, prior to XRF analysis. Color of samples is an indicator of lithofacies assignment.

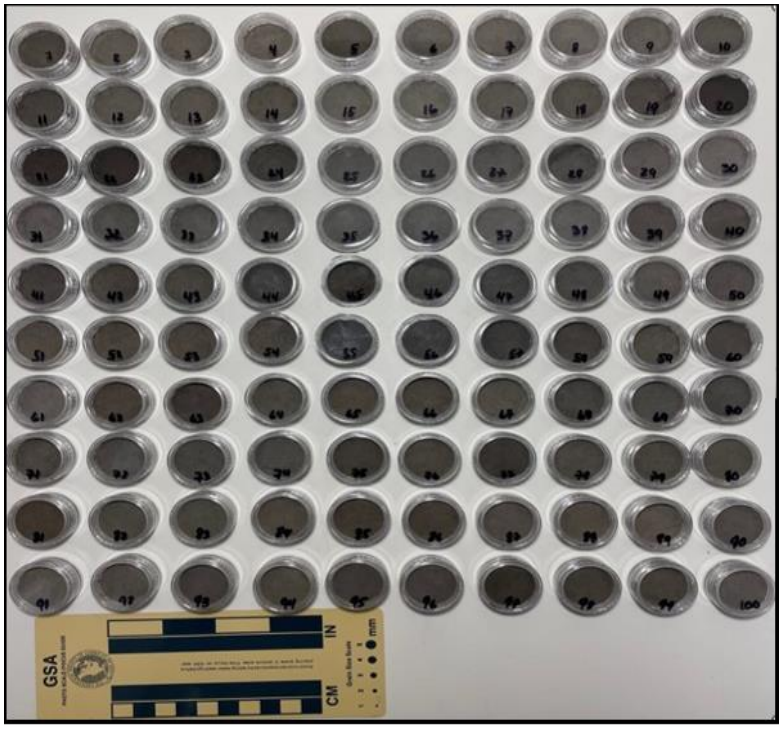

Figure 6. Drill cuttings analysis and mudlog over the Austin Chalk portion of the vertical well mudlog. Stratigraphic zonation of the chalk (zones A – E) are based on Ewing (2013) and correlated based on matching gamma ray signature.

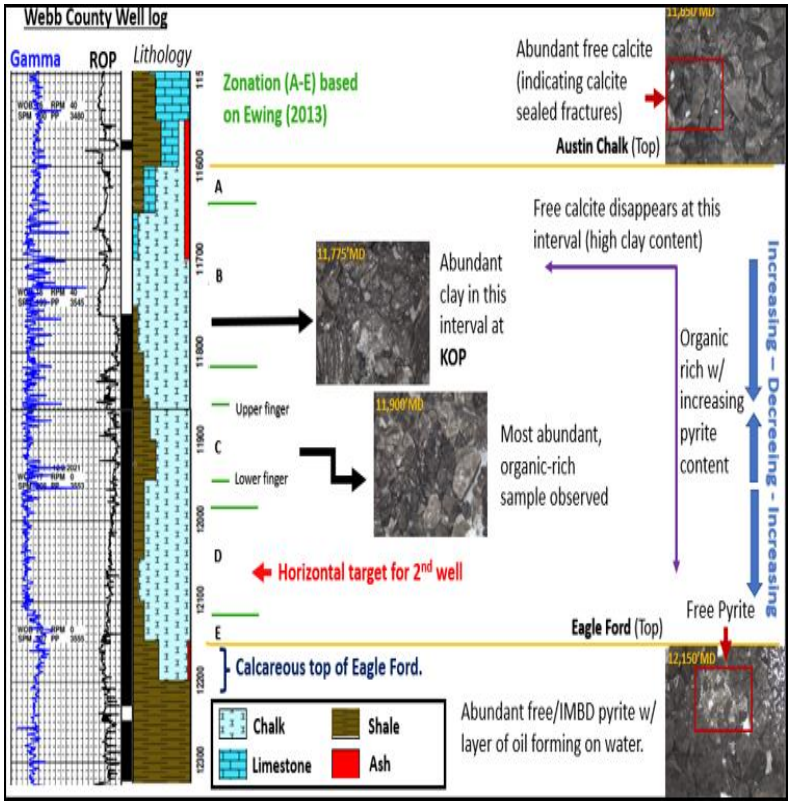

Figure 7. XRD analysis of drill cuttings in the vertical well. Calcite shown in blue, quartz in yellow, beryllium fluoride (Cristobalite) in white, and unidentified (clay mineral) peaks in pink. The dashed yellow curve indicates the probable values of quartz assuming a correctly assignment by the XRD match software.

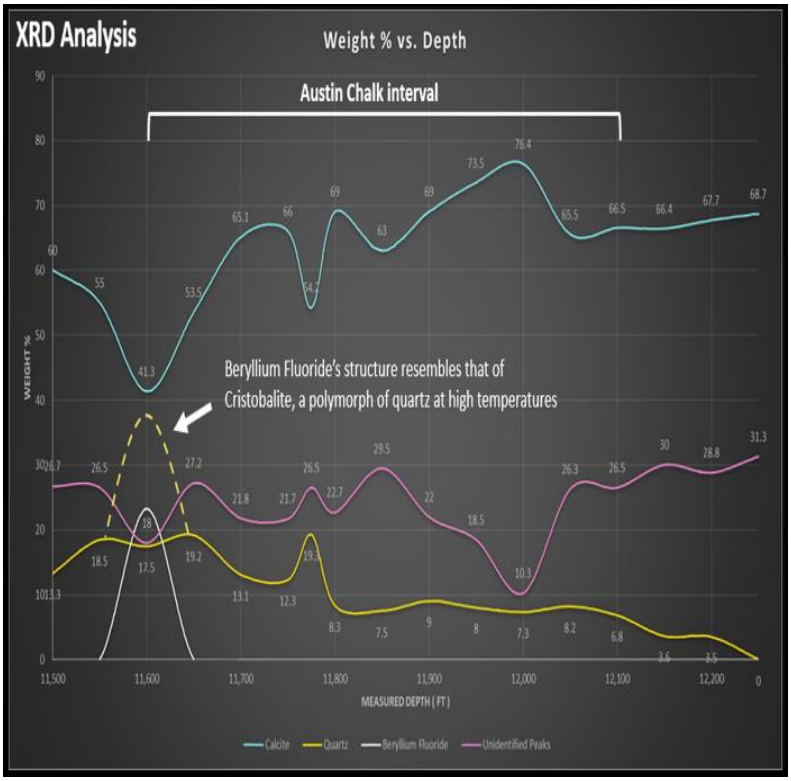

Figure 8. XRD analysis of drill cuttings in the vertical well, depicting the clay-rich interval seen at the kick-off point of the well on the mudlog. This interval occurs at the sequency boundary of unconformity, where the Lower Santonian section is missing. The decrease in quartz after this interval can be caused by less volcanism or be more biogenic in nature. Quartz values drastically decrease at the start of OAE 3.

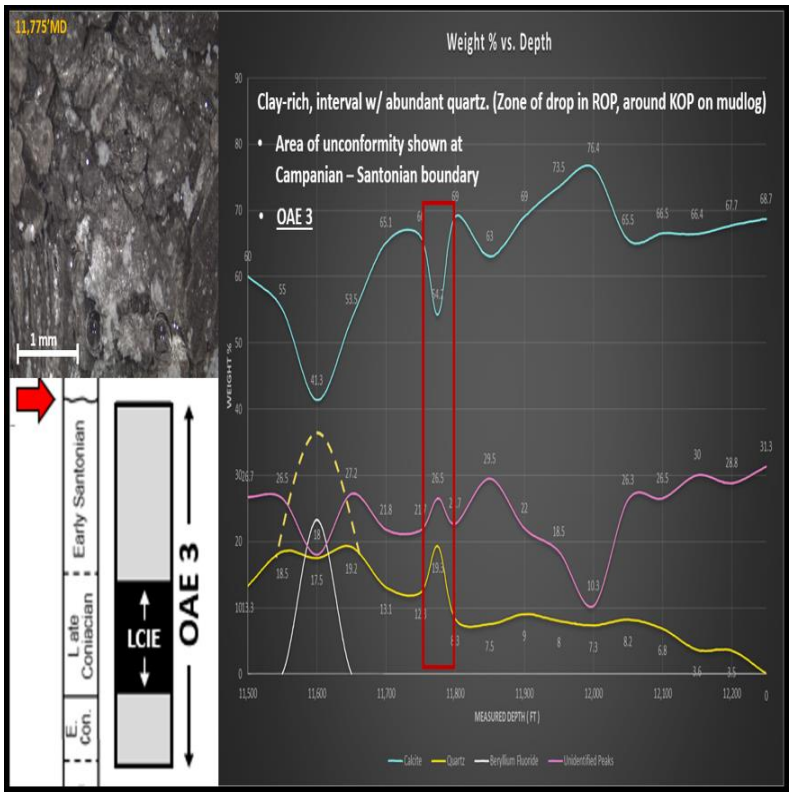

Figure 9. Mudlog of the vertical well plotted against the XRD analysis of drill cuttings. Cristobalite is present in the volcanic portion of the Austin Chalk. Target for the horizontal well is shown with red arrow, and resides within Zone D, the most organic-rich portion of the chalk.

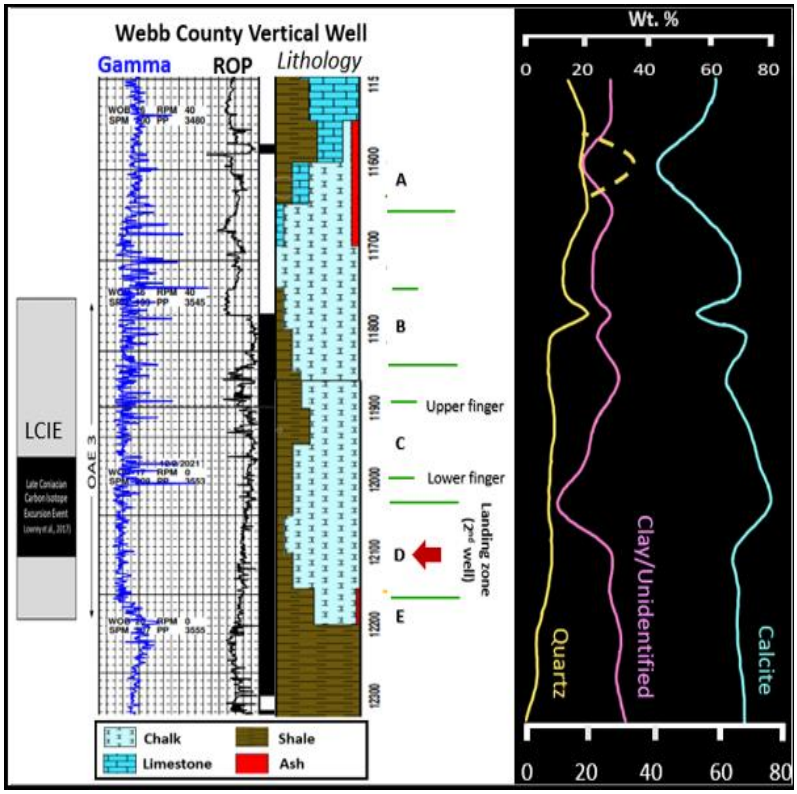

Figure 10. Lateral XRF analysis of the horizontal well, projected on a well trajectory, with total gas at the top. This information was pulled from the geosteering report supplied by the operator. Calcite, silica, and aluminum values are shown as weight precents, with interpreted faults from seismic data projected on well trajectory.

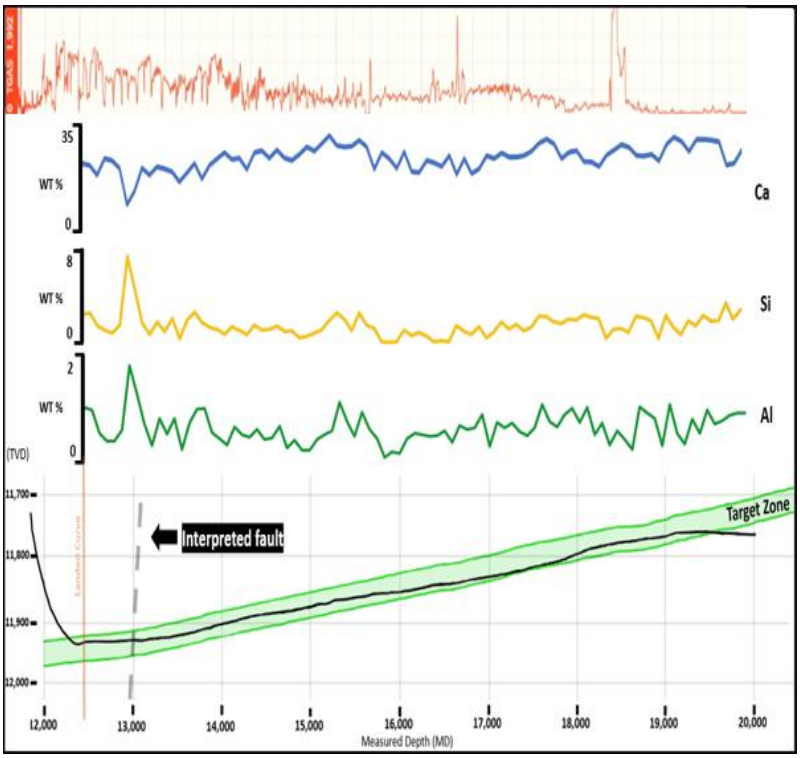

Figure 11. XRF analysis of the horizontal well, projected on a well trajectory, with total gas indicated in red at the top. This information was derived from the geosteering report supplied by the operator. Vanadium, copper, and nickel values are shown in parts per million (ppm), with interpreted faults from seismic data projected on well trajectory.

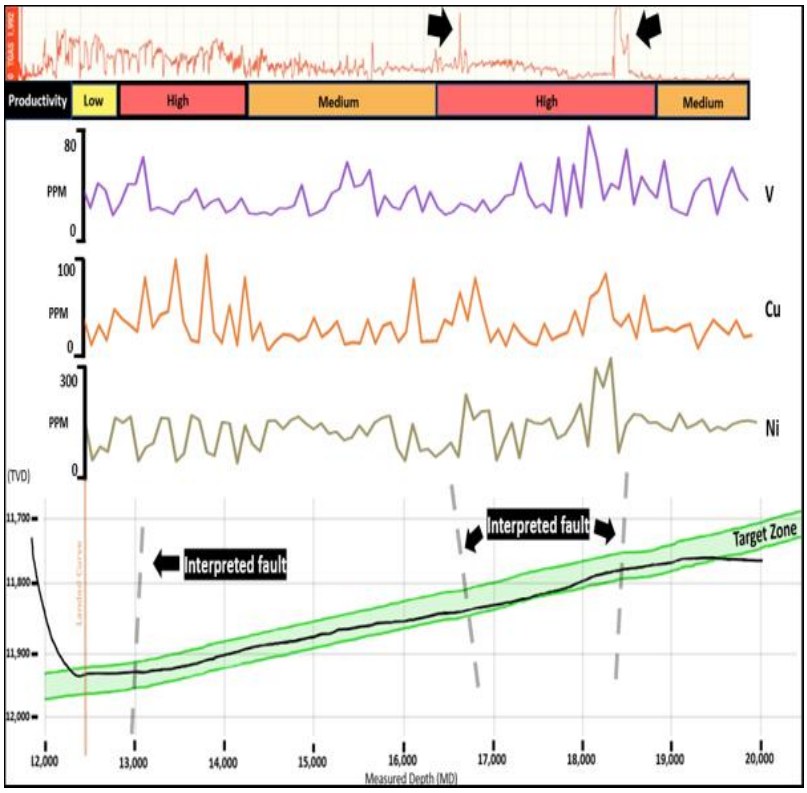

Figure 12. XRF analysis of the horizontal well, projected on a well trajectory, with total gas indicated in red at the top. This information was derived from the geosteering report supplied by the operator. Molybdenum, thorium, and nickel values are shown in parts per million (ppm), with interpreted faults from seismic data projected on well trajectory.

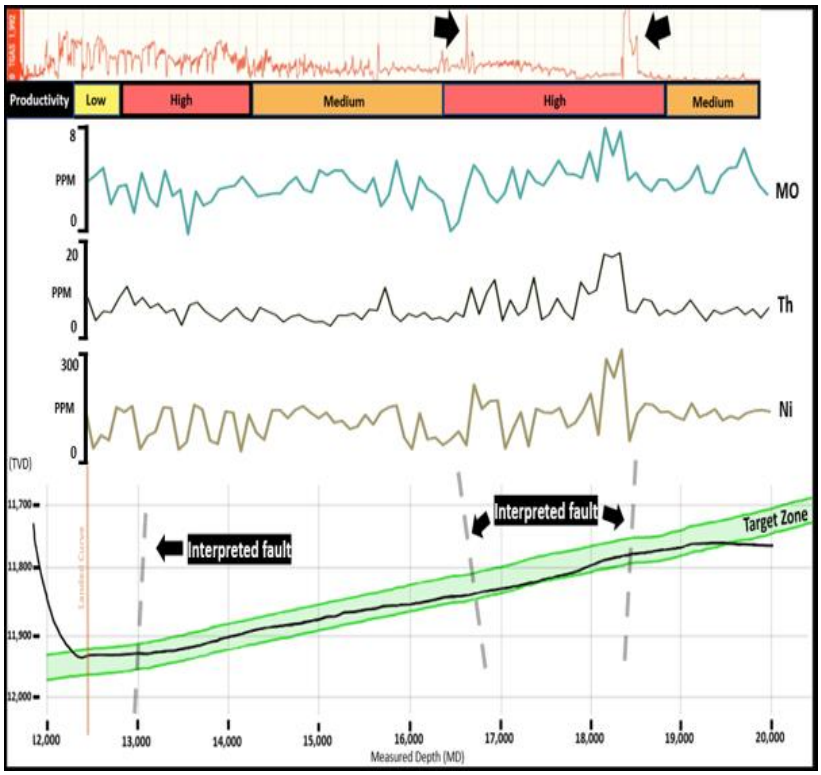

Figure 13. XRF analysis the horizontal wll, projected on a well trajectory, with total gas shown in red at the top. This information was derived from the geosteering report supplied by the operator. Silica values are shown in weight percent, while iron and sulfur values are shown in parts per million (ppm). Interpreted faults from seismic data projected on well trajectory.